Aquacultural Engineering 74 (2016) 30–37

Contents lists available at ScienceDirect

Aquacultural Engineering

journal homepage: www.elsevier.com/locate/aqua-online

Intrinsic settling rate and spatial diffusion properties of extruded fish feed pellets

Kristoffer Rist Skøien[a,*], Turid Synnøve Aas[b], Morten Omholt Alver[a,c], Odd Helge Romarheim[d], Jo Arve Alfredsen[a]

[a] Department of Engineering Cybernetics, Norwegian University of Science and Technology (NTNU), O. S. Bragstads plass 2D, NO-7491 Trondheim, Norway
[b] Nofima, Sjølsengvegen 22, NO-6600 Sunndalsøra, Norway
[c] SINTEF Fisheries and Aquaculture, NO-7465 Trondheim, Norway
[d] Nofima, NO-5828 Bergen, Norway

ARTICLE INFO

Article history:
Received 29 January 2016
Received in revised form 29 April 2016
Accepted 5 May 2016
Available online 10 May 2016

Keywords:
Atlantic salmon (*Salmo salar*)
Aquaculture
Extruded feed pellets
Pellet distribution modelling
Pellet settling rate and diffusion

ABSTRACT

Spatial and temporal feed distribution in sea cages are important factors for the farmer, fish and environment due to the strong relation to growth, feed loss, pollution and welfare. This study presents a set of experimentally derived diffusion parameters and settling rates obtained in still water from four sizes and three densities of extruded fish feed pellets commonly used in aquaculture. It was found that pellet size is positively correlated with increased diffusion and that pellet density plays a less important role. Both the size and density of pellets had a significant impact on the settling rate. Results are compared to values obtained during feed production as well as other relevant studies. The findings suggest that parameters related to hydrodynamic behaviour of groups of feed pellets may vary across different pellet types. The results may be applied to refine and parameterize pellet motion in sea cage feeding models, improving estimates of fish behaviour, growth and feed loss.

1. Introduction

Salmon (*Salmo salar*) farming is rapidly expanding across the world with global production of just 297 tonnes in 1970 compared to over 2,087,000 tonnes in 2013 (FAO, 2015). Production has moved from moderately sized cages owned by small companies to a consolidated industry with large production sites over the last decades. Cages are usually rectangular with 20–40 m sides and 20–35 m depth, or circular with a circumference of 90–157 m up to 48 m depth (Oppedal et al., 2011). In Norway, a single cage may hold up to 200,000 fish yielding a biomass of 1000 tonnes at an typical average slaughter weight of 5 kg. A daily feed ration of 1% (Oehme et al., 2012) corresponds to 10 tons of feed per cage per day. The expenditure on feed amounts to roughly 50% of all costs in Norwegian salmon and trout farming (Norwegian Directorate of Fisheries, 2013). With the feed loss from commercial farms estimated to around 7% (Gjøsæter et al., 2008), wasted feed is a substantial economic loss for the farmer as well as poor utilization of marine and plant resources (Alfredsen et al., 2007). Feed loss may in addition have a negative impact on the surrounding marine environment. Wild fish are drawn close to the cage enabling transmission of diseases between farm sites (Dempster et al., 2009) and large amounts of wasted feed in their diet can cause changes in their filet quality (Fernandez-Jover et al., 2007).

Feed waste is one concern, but the spatiotemporal distribution of pellets within the cage is also an important parameter for the fish. Giving easy feed access for the fish by utilizing the cage volume is desirable and is likely to promote rapid growth. The spatial and temporal distribution of pellets and ration size are key factors concerning feed availability (Juell, 1995) and these factors should not be confined so the fish may forage in an unrestricted manner (Talbot et al., 1999). The spatial distribution of pellets has a considerable influence on equal feed access (Attia et al., 2012) and localized feed delivery permits resource monopolization by dominant or competitive individuals, restricting feed access to subordinates (Juell, 1995; Ryer and Olla, 1996) causing greater size variation across the population (Johansen and Jobling, 1998). Suboptimal feed intake leads to both reduced and inefficient growth in Atlantic salmon (Einen et al., 1999). Aggressive behaviour and fin damage related to feed access have been demonstrated in a range of Salmonidae (Brännäs et al., 2005; Fenderson et al., 1968; Jobling, 1985; Noble et al., 2007, 2007, 2008; Rasmussen et al., 2007; Symons, 1971; Talbot et al., 1999) and summarized by Attia et al. (2012), Ruzzante

* Corresponding author at: Department of Engineering Cybernetics, Norwegian University of Science and Technology (NTNU), NO-7491 Trondheim, Norway.
E-mail address: kristoffer.rist.skoien@itk.ntnu.no (K.R. Skøien).

http://dx.doi.org/10.1016/j.aquaeng.2016.05.001
0144-8609/

(1994) and Talbot (1993), and this aggression is in turn related to injuries and mortality (López-Olmeda et al., 2012). Optimizing the spatiotemporal pellet distribution could thus result in considerable economic, environmental and welfare benefits.

To achieve these goals more knowledge must be obtained on the interaction between the feed, fish and the environment, on which models may be created to enable simulation and optimization of feed delivery.

In Norwegian salmon farming, feed is presented to the fish in the form of cylindrical pellets where the diameter is adapted to the size of the fish, normally from 3 to 12 mm diameter (Skretting, 2012) during the ongrowth in the sea. Feed pellets are commonly produced using an extrusion process. The extrusion system has a preconditioner which mixes water and steam into the dry ingredients in order to obtain a uniformly moisturized and preheated mix for the extruder barrel (Sørensen, 2012). This barrel housing may contain one or two rotating screws which mixes and transports the feed. The heated mix obtains its final pellet shape by being forced through a die plate and cut to length by a rotating knife (Sørensen, 2012). The pellets are dried and oil is finally added to increase the energetic content and obtain the desired density of the pellets. On farms feed is conveyed from large silos onboard a barge using compressed air to propel pellets through a pipe to a rotary pneumatic spreader located on the surface in the centre of the sea cage. Pellet transport, spreader rotation and pellet throw is driven by the same airflow.

For reference, the term settling rate refers to the intrinsic sinking speed of pellets, diffusion describes how random motion causes pellets on average to move from an area of high concentration to low concentration and advection is the motion of pellets caused by the bulk motion of the surrounding water. Above surface, Oehme et al. (2012) performed the first experiment which characterized the spatial pellet distribution from a rotary spreader by collecting pellets in Styrofoam boxes on the surface. Numerical models of the spreader have also been derived to investigate effects of different designs and wind (Skoien et al., 2015, 2016). For the pellet distribution below the surface an initial numerical model was developed by Alver et al. (2004) and has since been extended with a fish behaviour and foraging model (Føre et al., 2009). The combined model has been further developed and takes into account a range of factors such as the pellet distribution pattern across the surface, pellet size and settling rate, feeding rate, water flow and temperature. It also accounts for the fish properties with respect to motion, biomass and size distribution, appetite/satiation, foraging pattern and behaviour (Alver et al., 2016).

In Alver et al. (2004, 2016) the pellet concentration of a sea cage was modelled using the transport equation to describe the spatiotemporal dynamics of its distribution.

$$\frac{\partial c}{\partial t} + v_x \frac{\partial c}{\partial x} + v_y \frac{\partial c}{\partial y} + (v_z + u_v)\frac{\partial c}{\partial z} + \kappa \left(\frac{\partial^2}{\partial^2 x} c + \frac{\partial^2}{\partial^2 y} c + \frac{\partial^2}{\partial^2 z} c \right) = u - f_I \quad (1)$$

According to Alver et al. (2016), $c(x, y, z, t)$ is the feed concentration in the coordinate system given by the horizontal plane x, y, the vertical axis z and time respectively. $v_x(x, y, z, t)$, $v_y(x, y, z, t)$ and $v_z(x, y, z, t)$ are the individual orthogonal components of the water flow, u_v is the settling rate of the pellets, κ is the diffusion factor, $u(x, y, z, t)$ is the added feed and $f_I(x, y, z, t)$ the ingestion rate of the fish at a given position and time. In the present experiments, there is no water flow or fish. Eq. (1) can thus be simplified to Eq. (2).

$$\frac{\partial c}{\partial t} + u_v \frac{\partial c}{\partial z} + \kappa \left(\frac{\partial^2}{\partial^2 x} c + \frac{\partial^2}{\partial^2 y} c + \frac{\partial^2}{\partial^2 z} c \right) = u \quad (2)$$

It is not the intention of the present study to give a detailed account of the model as a comprehensive description can be obtained from Alver et al. (2004, 2016). Both κ and u_v which are parameters of essential importance have been determined based on the findings in the current study.

Limited research has been conducted with regards to characterizing the intrinsic diffusion properties of extruded fish feed pellets. This results in a range of sea cage and deposition models such as (Alver et al., 2004; Cromey et al., 2002, 2009; Gillibrand and Turrell, 1997) being based on alternative data as opposed to experimentally derived parameters from representative feeds. There has, however, been performed extensive research in determining the vertical settling rate u_v for various fish feeds (Chen et al., 1999; Cromey et al., 2002, 2009; Findlay and Watling, 1994; Sutherland et al., 2006). There may be several factors and interactions influencing diffusion. Heavier pellets may diffuse less simply because they will be suspended in the water column for a shorter period of time compared to a lighter pellet. However, a stronger relationship may be governed by a relation between size and increased diffusion due to greater settling rate and thus a higher level of erratic motion. It is also likely that density as well as size affects the settling rate due to the non-linear relationship between surface area/mass across different sized pellets.

The contribution of this study is a description of the pellet settling rate and diffusion process obtained through experiments involving a range of pellet types with different characteristics. These results may be of importance in determining central parameters in any feeding model involving pellets. The horizontal diffusion and vertical settling rate characteristics have been derived from the same pellets giving added benefit of matched data describing the motion of a pellet along all three axes. The results have been applied to the model described by Alver et al. (2016) to improve the estimation of the spatial and temporal pellet distribution.

2. Materials and methods

The work described in this study has been conducted as two separate experiments denoted the diffusion experiment and the settling rate experiment. The former quantifies the natural diffusion of pellets in the horizontal x, y plane released from a single point until they settle on the bottom. The latter is an extensive investigation of the settling rate and the vertical (z-axis) distribution of pellets dropped from an altitude, similar to being distributed by a rotary spreader. The diffusion and settling rate experiment are described in Sections 2.2 and 2.3 respectively.

2.1. Pellet properties

The experimental pellet types were produced at Nofima Feed Technology Centre, Bergen, Norway. Four different pellet sizes of {3, 6, 9, 12} mm diameter and cylindrical shape were produced to cover a wide range commonly used in Atlantic salmon farming. Each of the four pellet sizes were coated with three different amounts of oil to obtain pellets of low, medium and high density {L, M, H}, giving a total of twelve different pellet types. Each type is denoted by its pellet size and density, e.g. *9M* denotes a 9 mm pellet of medium density. The diet formulation was similar to the average Norwegian salmon feed in 2010 (Ytrestøyl et al., 2011). One basal mix of the dry feed ingredients was made and divided into four batches prior to extrusion. The four batches were processed with similar conditions in a Wenger TX52 extruder (Wenger, KS, USA), but with die plate holes of 2.5, 4.5, 7.2 and 10.0 mm diameter. The cutting knife speed was, however, adjusted for each production to ensure pellets with a length:diameter ratio of approximately 1:1. The pellets were dried to 92% dry matter in a hot air dual layer carousel dryer (Paul

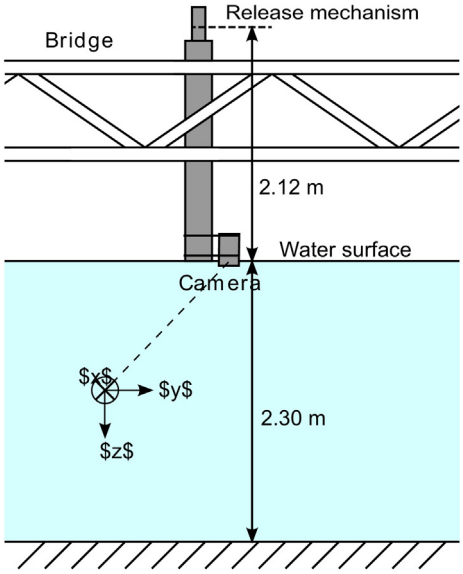

Fig. 1. The setup for the horizontal distribution experiment. Guide pipe attached vertically to a bridge crossing the tank. On top of the pipe is the quick release mechanism and the camera is mounted on the opposite end, barely breaching the water surface. The aluminium sheet is placed on the bottom of the tank. The origin of the global coordinate system is defined at the principal point of the camera, relocated in the figure for clarity.

Klöckner, Nistertal, Germany). Then each of the diets were coated in an experimental vacuum coater (Pegasus PG-10VC LAB, Dinnissen B.V., The Netherlands) with an oil blend of 43% rape seed oil and 57% fish oil. The low density diets were added an amount of oil giving slow sinking pellets, the high density diets were added the maximum amount of oil and the intermediate density diets were added an oil level halfway between the other two.

Pellet settling rate was measured at production based on 20 pellets released in a standing transparent cylinder (15 cm diameter, 1.7 m high) filled with 32 ppt NaCl salt water holding 20 °C. The measurement was started when the pellet was 5 cm below the water surface and the settling rate was calculated from the time it took a pellet to sink 1 m (Table 1). Bulk density was measured by weighing loosely poured coated pellets in a 1000 ml measuring cylinder (Table 1). Due to the differences in stacking efficiency, particle densities can not be directly compared. Diameter and length of the pellets were measured with an electronic caliper (Table 1) based on 20 pellets from each pellet size.

2.2. Horizontal distribution

The horizontal diffusion experiment was conducted at Nofima, Sunndalsøra, Norway, in a 7 m diameter octagonal 100 m^3 indoor seawater tank (Fig. 1). The x and y axes are horizontal and points towards the edges of the tank, and z points downwards. The tank bottom sloped slightly from the edge towards the drain located at the centre of the tank. Water flow was measured at 0.2, 1.2 and 2.2 m depth in both x and y direction with a propeller anemometer (0.00 m/s, handheld flow meter HFA and vane wheel, Höntzsch, Waiblingen, Germany) performed prior to experiments to ensure that the water mass was stationary. Although the water was stationary, surface particles displayed some minor motion which was attributed to the airflow from the ventilation system. The salinity was measured to 31.7 ppt (Cond 330i with a TetraCon conductivity measuring cell, WTW – Wissenschaftlich-Technische Werkstätten GmbH, Weilheim, Germany). With $T = 12$ °C, the water density was calculated to 1024 kg/m^3 Pond and Pickard (1983, pp. 310).

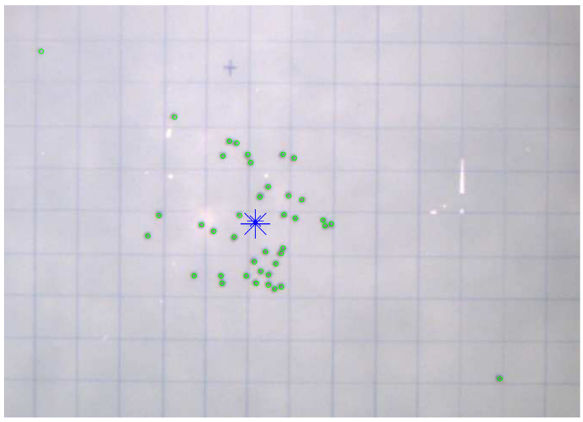

Fig. 2. Analysis of one drop of *6H* pellets superimposed on the cropped original image. All 40 pellets have settled in this drop. Circles indicate the manually marked pellet positions, the large asterisk is the centre of mass, and the small asterisk is centre of pipe projected down onto the target. Two of the pellets are far from the centre of mass probably due to surface drift before sinking.

The pellets were placed in a 70 mm diameter vertical pipe equipped with a quick release mechanism (Fig. 1). The pellets were concurrently released and guided to the water surface by an 80 mm diameter pipe ending at the surface. This resulted in a total distance from release position to water surface of 2.12 m. Disregarding friction against the pipe wall and aerodynamic resistance, this yields a free-fall time of 0.657 s from release to water impact at a rate of 6.45 m/s obtained from basic equations of motion. From the surface, pellets travelled 2.30 m through the water column before settling on a 1.00 × 1.00 m sheet of aluminium with a 50 × 50 mm grid on the bottom of the tank. A digital camera (FL3-GE-13S2C-CS, Point Grey Research, Inc., Richmond, Canada) equipped with an adjustable lens (M13VM308, Tamron Co., Ltd, Saitama-city, Japan) encapsulated in a waterproof housing was mounted at the end of the 80 mm pipe, capturing an image of the settled pellets at the end of each drop. Five replicate drops of 40 pellets each were conducted for each of the 12 pellet types, giving a total of 60 drops conducted in randomized order. There were some observations of pellets that remained afloat for an indefinite period of time or sunk later, long after the main bulk of pellets. This effect was mostly pronounced in the low density pellets. A drop was deemed finished and a picture captured as soon as there were no pellets sinking through the water column. The target grid was brushed clean of pellets after each image capture and the position of the target in relation to the pipe was verified by a laser cross and realigned if necessary. The water was left to settle for at least two minutes before the next drop was performed.

The images and pellet positions were analyzed using openCV (Bradski, 2000; MATLAB, 2014; SPSS, 2015). The position of each pellet was manually identified in the image obtained from each drop. The procedure of mapping from camera pixel coordinates $(\mathbb{R}^2)\ \boldsymbol{p} = \begin{bmatrix} u & v \end{bmatrix}^T$ to the world coordinate frame on the bottom $(_b)$ of the tank $(\mathbb{R}^2)\ \boldsymbol{q} = \begin{bmatrix} x_b & y_b \end{bmatrix}^T$ was performed by establishing the homography matrix $\boldsymbol{H}$ and calculating the transformation using the augmented vectors $\tilde{\boldsymbol{q}} = \boldsymbol{H}^{-1}\tilde{\boldsymbol{p}}$. $\boldsymbol{H}$ was obtained from a calibration image from which nine central grid points were extracted and $\boldsymbol{H}$ calculated by using the MATLAB toolbox from Corke (2011) yielding a residual of 0.89. An image example can be seen in Fig. 2.

For the purpose of statistical analysis it is assumed that there is an isotropic bivariate distribution around the centre of mass for the group of settled pellets. The centre of mass on the bottom of the tank was defined as zero $\bar{x}_b = 0$ and $\bar{y}_b = 0$ for each drop. Comparing the centre of mass to the pipe centre projected onto the bottom reference grid verifies that centre of mass was located close to pipe

Table 1
Settling rate mean ± SD [cm/s] measured in a vertical cylinder at production (N = 20, 20 °C water, 32 ppm NaCl), bulk density at production, mean ± SD [g/l] (N = 3 replicate measurements for 3 and 6 mm, N = 4 for 9 and 12 mm), oil content [%]. Diameter and length, mean ± SD [mm] of pelleted feed at production (N = 20).

		3 mm	6 mm	9 mm	12 mm
Settling rate	*H*	10.2 ± 0.5	11.8 ± 0.9	14.7 ± 0.8	16.6 ± 1.6
	M	8.1 ± 0.6	6.4 ± 1.5	10.7 ± 2.5	12.4 ± 2.4
	L	5.9 ± 1.2	5.3 ± 1.2	7.8 ± 1.5	9.7 ± 1.7
Bulk density	*H*	706 ± 7	671 ± 15	673 ± 7	637 ± 17
	M	645 ± 5	596 ± 16	623 ± 3	597 ± 5
	L	583 ± 4	556 ± 19	582 ± 11	567 ± 9
Oil content	*H*	21.0	28.0	30.0	32.0
	M	13.0	22.5	25.0	27.5
	L	5.0	17.0	20.0	23.0
Diameter		3.0 ± 0.1	6.0 ± 0.1	9.4 ± 0.2	12.8 ± 0.2
Length		3.8 ± 0.5	6.4 ± 0.4	9.0 ± 0.4	12.6 ± 0.7

centre, as is expected when there is no water flow present. The radial distance r_b from $\bar{x}_b$, $\bar{y}_b$ to each pellet was calculated for each drop. The vector $\boldsymbol{r}_b$ contains measured radial distances of pellets of a single type which has a Rayleigh distribution, assuming that all the x_b and y_b distances has zero mean, are normally distributed, independent and with equal variance (Forbes et al., 2011).

In the captured images it was evident that some pellets came to rest far from the centre of mass of the main cluster, as in Fig. 2. This observation was attributed to odd low-density, oddly shaped or pellets that got an air bubble attached to their surface. The latter made certain pellets float for a period of time exposing them to the previously mentioned slight surface motion caused by the ventilation system. To counter this effect, the image was captured as soon as there were no sinking pellets in the water column. However, some pellets affected by surface motion were unavoidably part of the captured image. To further limit this adverse effect, outliers were removed by visually inspecting the histogram of $\boldsymbol{r}_b$ and comparing it to a Rayleigh probability density function fitted to the data by the MATLAB command `fitdist`. This procedure defined 50 pellets (2.4%) as outliers of a total 2116 and removed them from the analysis. Small and low density pellets appeared more prone to have outliers.

For significance testing a one-way ANOVA was applied to the data set. Two-way ANOVA was not used since the particle density may be unequal for pellets of different size. $\boldsymbol{r}_b$ was square root transformed for all the pellet types and scaled so the minimum value is anchored at unity as according to (Osborne, 2002). 21 outliers were detected by box plot inspection (data points greater than 1.5 box-lengths from the edge). However, there were no extreme outliers and all outliers were situated close to the box. Some of these outliers may have been caused by one of the aforementioned reasons but they were kept in the data set as there was no clear radial separation from the remainder of the data. Normality was assessed using the Shapiro–Wilk test and found to be violated for 3*H*, 3*M*, 6*M* and 9*L* ($p < .05$). Since the group size for these four pellet types are large, (200, 198, 146 and 167 respectively), a Q–Q plot analysis was carried out as well which indicated fairly normally distributed values. The overall histogram shapes of $\sqrt{\boldsymbol{r}_b}$ looks similarly shaped, mostly with a slightly positive skewness. However, due to the robustness of ANOVA the analysis was still performed using this method. Assumption of homogeneity of variances was not satisfied which was assessed by Levine's test ($p < 0.0005$), hence, the remainder of the analysis was performed with a Welch ANOVA.

2.3. Settling rate

The vertical settling rate experiment was conducted in a cylindrical indoor tank 2.76 m high, 0.79 m diameter filled with fresh water. Sea salt was added and the salinity and temperature measured using a CTD probe (SonTek CastAway, CA, USA). Salinity and temperature readings were taken across the entire depth of the tank at three different times during the experiment. Salinity varied from 28.9 to 33.2 ppt (average 32.0 ppt), generally increasing with depth. Temperature ranged from 17.2 to 17.9 °C (average 17.6 °C). Using the average readings the water density was calculated to 1023 kg/m^3. The vertical guide pipe and release mechanism were the same as in the horizontal diffusion experiment described in Section 2.2. A camera and lens configuration as described in Section 2.2 was enclosed in a watertight housing and mounted horizontally, capturing images of passing pellets at a depth of 2.30 m. This device was positioned at the bottom of the tank and aimed towards a uniformly backlit surface where the camera captured high contrast images of pellets traversing the field of view. To guide pellets into the field of view, a 135 mm high funnel was attached to the rig giving a detection area of approximately 0.1 m^2, equivalent to 17% of the cross sectional area of the tank. This device is further detailed in Skøien et al. (2014). The camera was configured to output images of 640 × 480 pixels, 8 bit grayscale at 56 frames per second. Images were continuously transferred through an Ethernet and power umbilical and stored with a timestamp on a local computer.

Ten replicates of each pellet type were dropped in randomized order. Due to the large number of pellets, the individual pellet containers were measured by volume and 3, 20, 70 and 230 ml of 3, 6, 9 and 12 mm pellets respectively were used. The volumes were experimentally determined to provide a high number of pellets passing the sensor while keeping manual quantification manageable. The release process was identical to the one in the diffusion experiment but there was no pause between drops as there was no need to introduce foreign objects into the body of water for cleaning purposes. The duration of the recorded video for a given pellet type was determined based on the settling rate measured at production (Table 1). Assuming a normally distributed settling rate, a drop was deemed finished when four standard deviations above the mean was reached. On the rare occasion that pellets were still present in the live video stream after this period of time, the recording was extended until pellets could no longer be observed.

The recorded video and corresponding timestamps were analyzed utilizing a C++ and OpenCV (Bradski, 2000) implementation. The software traversed the video stream frame by frame with an operator signaling when a pellet passed a fictive horizontal line in the image corresponding to a depth of 2.30 m, identical to the diffusion experiment. From this the settling rate was calculated for each pellet and the results analyzed across all replicates of the 12 pellet types.

A one-way ANOVA was used for significance testing using the transformed data set using reflect and $\log_{10}$ ($\log_{10}$(max(data) + 1-data). Some outliers were present in the data but these could

Table 2
Number of pellets settling on the tank floor including pellets later classified as outliers for each pellet type. Numbers in parenthesis indicates average per replicate. <40 indicates the presence of positively buoyant pellets, >40 indicates breakage or other debris present in the image.

	3 mm	6 mm	9 mm	12 mm
H	206 (41.2)	200 (40.0)	198 (39.6)	193 (38.6)
M	202 (40.4)	152 (30.4)	198 (39.6)	193 (38.6)
L	196 (39.2)	49 (9.8)	172 (34.4)	157 (31.4)

Table 3
Average distance from centre of mass, mean ± SD [mm]. Number of pellets analyzed with outliers removed. The rightmost column indicates pellet types between which significant differences could not be established at $p < 0.05$ in relation to all other types based on results of Games–Howell analysis from the transformed data: $\sqrt{\boldsymbol{r}_b}$.

Pellet type	Mean distance [cm] ($\bar{\boldsymbol{r}}_b$)	*N*	No. Sig. difference
3H	61 ± 43	200	*3M, 3L, 6H*
3M	61 ± 48	198	*3H, 3L, 6H*
3L	70 ± 40	191	*3H, 3M, 6H, 6M, 6L,*
6H	68 ± 40	197	*3H, 3M, 3L, 6M*
6M	80 ± 57	146	*3L, 6H, 6L, 9H, 9M, 9L*
6L	89 ± 57	48	*3L, 6H, 6M, 9H, 9M, 9L, 12L*
9H	92 ± 48	198	*6M, 6L, 9M, 9L*
9M	93 ± 49	197	*6M, 6L, 9H, 9L*
9L	95 ± 64	167	*6M, 6L, 9H, 9M*
12H	130 ± 70	189	*12M, 12L*
12M	140 ± 76	190	*12H, 12L*
12L	119 ± 61	145	*6L, 12H, 12M*

not be attributed to either data entry or measurement errors and were hence included in the study. Assessment of normality was performed using the Shapiro–Wilk test and found that 5 pellet types did violate the assumption of normality at $p < 0.05$. However, the ANOVA is not highly sensitive to normality deviations (McDonald, 2014). Inspection of the histograms indicated reasonable normality with mostly positive skew and some types slightly negative skewed. As stated by McDonald (2009), the one-way ANOVA is more powerful compared to the non-parametric Kruskal–Wallis test and ANOVA should be used except when the data is severely non-normal. Homogeneity of variances was tested using Levine's test and found violated at $p < 0.0005$, thus Welch ANOVA was used for the analysis.

3. Results

3.1. Production measurements

Table 1 presents the measurements obtained from Nofima Feed Technology Centre, Bergen, Norway, during feed production. These results will act as a reference for the main experiments in this study and will not be discussed in detail.

3.2. Horizontal diffusion

The number of pellets settling on the bottom and becoming part of the captured images are presented in Table 2. The average number of pellets sinking and settling on the bottom for each type was between 30.4 (76% of the 40 pellets) and 41.2 (103%), except from *6L* at 9.8 (25.5%). Across all sizes the number of pellets settling on the tank floor was positively correlated with density. In some cases the number of counted pellets exceeded 40 which was due to breakage and difficulty in separating intact pellets from fragments during the analysis. This issue was only evident the 3 mm pellet types.

As seen in Table 3, across pellet types the average radial distribution increased with size across all densities with one exception of *6H* at 68 cm which is slightly less than *3L* at 70 cm.

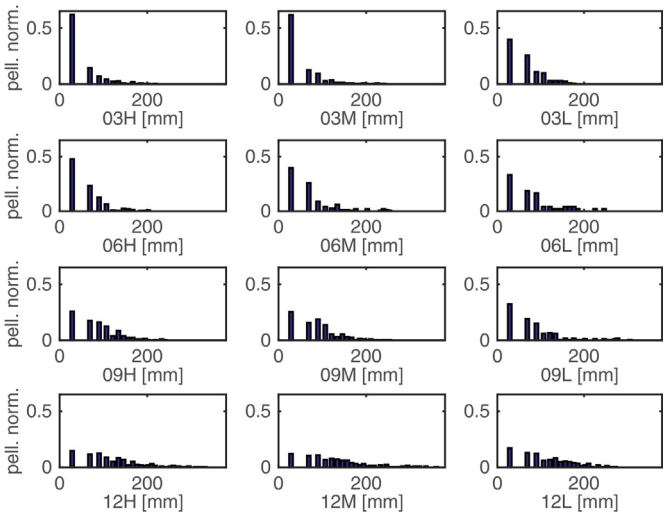

Fig. 3. Number of pellets in each annulus for each of the twelve pellet types. Each annulus and central circle are of equal area, and the number of pellets have been normalized. Distance from centre of mass in mm.

Table 4
The average and ±SD settling rate [cm/s] for all types and number of pellets analyzed. The rightmost column indicates difference in settling rate compared to the values measured at production.

Pellet type	Settling rate (u_v)	*N*	Diff. from prod.
3H	9.9 ± 0.5	506	−2%
3M	7.7 ± 0.8	435	−5%
3L	5.6 ± 1.0	376	−6%
6H	12.3 ± 0.9	329	4%
6M	8.1 ± 1.8	250	+27%
6L	6.2 ± 1.7	84	+18%
9H	14.0 ± 2.0	254	−5%
9M	12.8 ± 2.3	214	+20%
9L	9.7 ± 2.1	186	+24%
12H	17.0 ± 2.9	192	+2%
12M	14.2 ± 2.5	186	+14%
12L	11.3 ± 2.5	177	+16%

The statistical analysis stated that there were significant differences across $\sqrt{\boldsymbol{r}_b}$ for the 12 pellet types, Welch's $F(11, 667.228) = 39.859$, $p < .0005$. This result was followed up with a Games–Howell post-hoc test and the results are presented in Table 3.

To illustrate the diffusion of pellets, the radial distance $\boldsymbol{r}_b$ from each pellet to the centre of mass for the respective drop was concatenated across all five replicates. A circle with a radius of 380 mm was divided into 43 annuli with an additional circular central section all with equal area. Fig. 3 illustrates the normalized number of pellets in each annulus and central circle for each of the twelve pellet types.

From Fig. 3 and Table 3, diffusion was positively correlated with pellet size with the one exception of *6H* which diffused slightly less compared to *3L*. The 12 mm pellets stand out in the analysis as they in general diffused significantly more than the rest of the pellet types, with the exception of *12L* which is not significantly different from *6L*. Within the same sized pellets there is a tendency towards increased diffusion with reduced density with the exception of *12L*.

3.3. Settling rate

The average settling rates from the experiment are presented in Table 4 and corresponding normalized histograms are presented in Fig. 4. The settling rates ranged from 5.6 cm/s for *3L* to 17.0 cm/s for *12H*. Across all pellet types, increased density was positively

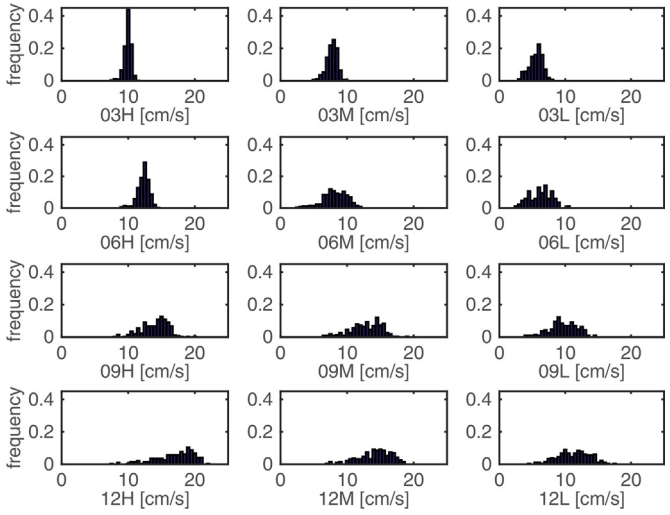

Fig. 4. Settling rate for each pellet type [cm/s], normalized count. Histograms plotted with 0.5 cm/s bin width.

correlated with settling rate. For pellets of identical density, there was also a positive correlation between size and settling rate. Upon inspection of Fig. 4 it seems that smaller pellets tend to settle as a uniform cluster whereas larger ones have a greater span in their settling rate. This observation is also evident from the standard deviations in Table 4. Comparing the settling rates from the experiment to those measured at production yields generally good correspondence. *3H*, *3M*, *3L*, *6H*, *9H* and *12H* all deviate no more than 6% from the production values. The remaining pellet types however have a faster settling compared to the production values, ranging from +14% to +27%.

Significant differences were detected between the transformed settling rates, Welch's $F(11, 916.393) = 1394$, $p < 0.0005$. Multiple comparisons were performed using the Games–Howell post-hoc test and found significant differences between all pellet types $p < 0.016$, with the exception from two pairs, *3H* and *9L* as well as *9H* and *12M*.

4. Discussion

As seen in Table 3 and the accompanying ANOVA analysis there was significant differences in the root radial diffusion $\sqrt{\bar{\boldsymbol{r}}_b}$ between pellet types. There were no significant differences in $\sqrt{\bar{\boldsymbol{r}}_b}$ between pellets of the same size ($p > 0.05$). Hence, it appears that pellet density is not a significant factor in determining diffusion. Since specific pellet density measurements were unavailable, the relation between this result with respect to specific density is unknown. However, between sizes the results differed greatly. These results suggest that modelling of pellet diffusion cannot be accurately represented by a generalization across all sizes and densities. However, within a given pellet size the distribution variability was limited, which may lead to satisfactory simulation results without considering the density of a given pellet type. This simplifies modelling as the pellet size is often readily available but the density may be more cumbersome to obtain. Note that the fat content described in Table 1 is not a descriptor for the specific density of a pellet. A larger pellet may expand more in percentage compared to a small pellet leaving more room for oil.

The conversion from image/pixel coordinates $\boldsymbol{p}$ to the world coordinate frame $\boldsymbol{q}$ was performed using the homography transform (Corke, 2011) based on 9 image points. This approach does not account for lens distortion but the fact that the field of view was narrow and the pellets settled close to the centre of the image greatly reduced any distortional effects. Visual inspection of the captured images showed minor distortion, which combined with the low residual value of the homography computation, gives satisfying credibility to the classification of the real life pellet positions. The $\bar{\boldsymbol{r}}_b$ in Table 3 may be used by modellers to verify that pellets originating from a point source in still water has the appropriate average Euclidean radial diffusion at 2.30 m depth. This may be achieved by adjusting the diffusion parameter, such as κ in Eq. (1). These values have already been incorporated in a sea cage model (Alver et al., 2016) for improved simulation accuracy. These parameters will likely become increasingly relevant when simulations are run under realistic conditions with a horizontal water flow field, especially for low density pellets. The slow settling rate will expose the pellets for a prolonged period of time before being eaten by fish or escaping the cage.

The obtained settling rates generally corresponded well with the values measured at production time. Interestingly, the smallest pellet types *3H*, *3M*, *3L* as well as all the high density types *6H*, *9H* and *12H* deviated no more than 6% either negatively or positively from the settling rate measured at production. For the medium and low density 6, 9 and 12 mm types, the smallest deviation from production values was 14% for *12M* and the largest deviation was 27% for *6M*. The largest differences occurred among the larger pellet types, *6M*, *6L*, *9M* and *9L* which showed positive deviations from the production measured settling rate, and *12M* and *12L* portrayed a smaller positive difference. This effect was not clearly understood. Factors which might contribute are (1) The fact that the entire cross-sectional area of the tank was not measured. Faster pellets may have travelled in the centre of the pellet cloud in the horizontal plane, resulting in a larger proportion of the faster pellets being measured. (2) The batch of pellets being released from altitude might give heavier pellets a boost compared to lighter ones. The simultaneous release of pellets was probably more realistic than single pellets measured in isolation when comparing it to a feed spreader which releases pellets in batches at 1–2 m above sea level. This though might explain the positive skew compared to the manufacturing results and the effect may be somewhat reduced if the tank was deeper.

The camera rig could not detect pellets across the entire cross sectional area of the cylindrical tank due to its limited field of view. The funnel on the camera rig accounts for the comparatively low N (Table 4) of pellet types with high diffusion as fewer of them passed the detection area. *6L* had a very low pellet count of 84 which is attributed to both a high diffusion factor as well as this particular pellet type being very buoyant with many floating pellets as was also observed in the diffusion experiment. The funnel height was only 135 mm and quite steep, which in comparison to the total settling distance is likely too modest to influence the settling rate measurements in a noticeable manner. However, such a delaying effect would manifest itself as a decrease in settling rate but the results were generally faster than the settling rates measured at production.

Inspecting the standard deviations in settling rates from Table 4 also reveals that the vertical spread of pellets increased with size. There is only one exception for ±1.0 cm/s for *3L* and ±0.9 cm/s for *6H*. This observation corresponds well with the diffusion experiment as larger pellets tended to diffuse more vertically as well as horizontally. This could be due to a positive correlation of chaotic motion and pellet size, or possibly that larger pellets have greater surface area which renders them susceptible to air bubbles attaching to the surface. A larger pellet may in turn capture either a small or a large volume of air, increasing the range of buoyancy.

Fig. 5 compares the results from the present study with production measurements as well as various feeds from Chen et al. (1999), Findlay and Watling (1994) and Sutherland et al. (2006). The agreement is quite good although the pellet types used in this study seem to have an overall slower settling rate. This effect may

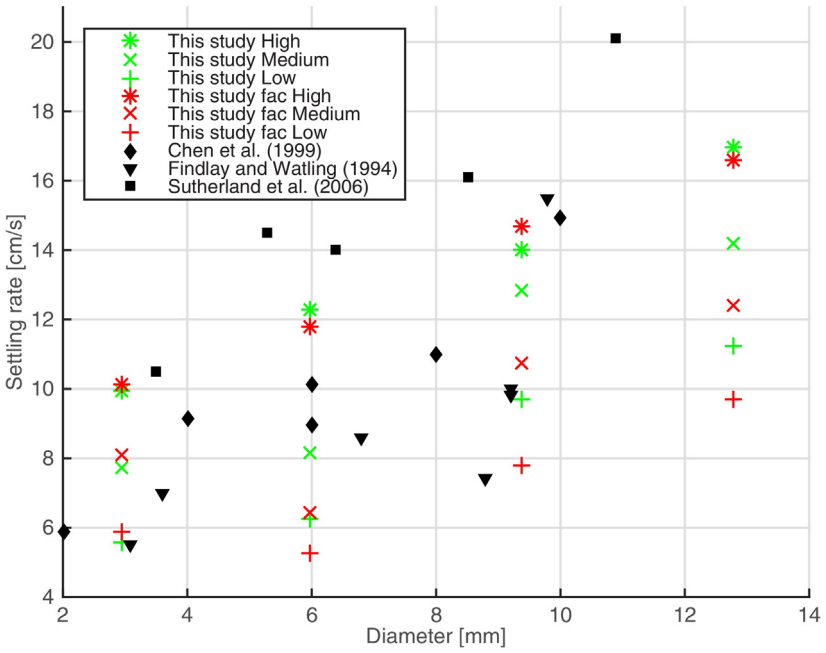

Fig. 5. Comparing settling rate and measured diameter. Comparison of experimental results, factory production measurements and studies by Chen et al. (1999), Findlay and Watling (1994) and Sutherland et al. (2006).

have been caused by the nutritional composition of the feed as well as the present pellets having a diameter/length ratio of approximately 1:1. Inspecting the results of Sutherland et al. (2006) which are overall faster, had a much lower diameter/length ratio. Pellets which are longer, more cylindrically shaped as opposed to the comparatively spherical ones used in this study may have a more stable orientation in the water column which may result in a faster settling rate. It should be noted that in Sutherland et al. (2006) their own comparison of settling rate against other pellet types showed that their pellets did indeed settle comparatively fast.

The pairwise significance analysis on the transformed data resulted in all pellet types having significantly different settling rate at $p < 0.05$ with the exception of the two pairs, *3H* and *9L* as well as *9H* and *12M*. Inspecting Table 4, other pellet types also showed very similar settling rates such as *3M* and *6M*. This may suggest that the data transformation increased the type I error rate and the significance analysis should be interpreted with caution.

For the modeller a recommendation would be to choose a suitable diffusion parameter from Table 3 based on the appropriate pellet size. As stated, no significant differences could be detected between identically sized pellet types so an average or median value might suffice. With respect to the settling rate, this value is often obtainable from the producer and should be used if available. Otherwise, a suitable settling rate from Table 1 or Table 4 could be chosen. The former table was taken from $N = 20$ at production and seems to settle slightly slower, but generally correspond well with other studies as presented in Table 5. The latter was taken from a much larger data set and released in a manner which is likely more realistic in relation to rotary spreaders in sea cage production. These results show an overall faster settling rate and these may have been more in line with the production measurements had the tank been deeper, possibly due to a faster settling rate at the shallowest section of the water column. From a pneumatic spreader, pellets will have a horizontal velocity component which has not been considered in this study. However, it is likely that this horizontal component will be quickly eliminated upon water impact and the intrinsic settling rate becoming the dominant velocity component in still water.

5. Conclusion

This study has examined the horizontal diffusion and settling rate based on experiments with four sizes and three densities of extruded salmon pellets under stationary water conditions. For horizontal diffusion only the pellet size had a significant impact on the radial distance from the centre of mass while both the size and density affected the settling rate. The results have been used to refine and parameterize a sea cage model (Alver et al., 2016) where pellet motion plays an essential role. These results allow for spatiotemporal pellet distribution and water flow induced motion to be more accurately modelled by hydrodynamics and equations of motion based on the presented experimentally derived parameters. These findings will expectedly yield improved model estimates of pellet motion within a sea cage, fish behaviour and feed loss.

Acknowledgments

Appreciation is extended to M.S. Klinge and R.E. Myrmel at Nofima for producing the experimental pellets, P.I. Snildal and T. Haugen at the Department of Engineering Cybernetics workshop at The Norwegian University of Science and Technology (NTNU) and F. Nerland at Nofima for assisting with the experiment. This research has been funded by the Centre for Research-based Innovation in Aquaculture Technology (CREATE) (Research Council of Norway, Grant number: 174842), SINTEF Sealab, NO-7645 Trondheim, Norway.

References

Alfredsen, J., Holand, B., Solvang-Garten, T., Uglem, I., 2007. Feeding activity and opercular pressure transients in Atlantic salmon (*Salmo salar* L.): application to feeding management in fish farming. In: Almeida, P., Quintella, B., Costa, M., Moore, A. (Eds.), Developments in Fish Telemetry. Developments in Hydrobiology, vol. 195. Springer, Netherlands, pp. 199–207, http://dx.doi.org/10.1007/978-1-4020-6237-7_19.

Alver, M.O., Alfredsen, J.A., Sigholt, T., 2004. Dynamic modelling of pellet distribution in Atlantic salmon (*Salmo salar* L.) cages. Aquacult. Eng. 31 (1–2), 51–72, URL http://www.sciencedirect.com/science/article/pii/S0144860904000056.

Alver, M.O., Skøien, K.R., Føre, M., Aas, T.S., Oehme, M., Alfredsen, J.A., 2016. Modelling of surface and 3D pellet distribution in Atlantic salmon (*Salmo salar* L.) cages. Aquacult. Eng. 72-73, 20–29, URL http://www.sciencedirect.com/science/article/pii/S0144860916300462.

Attia, J., Millot, S., Di-Poï, C., Bégout, M.-L., Noble, C., Sanchez-Vazquez, F., Terova, G., Saroglia, M., Damsgård, B., 2012. Demand feeding and welfare in farmed fish. Fish Physiol. Biochem. 38, 107–118, http://dx.doi.org/10.1007/s10695-011-9538-4.

Bradski, G., 2000. The OpenCV Library. Dr. Dobb's Journal of Software Tools.

Brännäs, E., Berglund, U., Eriksson, L.-O., 2005. Time learning and anticipatory activity in groups of Arctic charr. Ethology 111 (7), 681–692, http://dx.doi.org/10.1111/j. 1439-0310.2005.01094.x.

Chen, Y.-S., Beveridge, M.C., Telfer, T.C., 1999. Physical characteristics of commercial pelleted Atlantic salmon feeds and consideration of implications for modeling of waste dispersion through sedimentation. Aquacult. Int. 7, 89–100, http://dx.doi.org/10.1023/A:1009249721787.

Corke, P.I., 2011. Robotics, Vision & Control: Fundamental Algorithms in Matlab. Springer.

Cromey, C.J., Nickell, T.D., Black, K.D., 2002. DEPOMOD-modelling the deposition and biological effects of waste solids from marine cage farms. Aquaculture 214 (1–4), 211–239, URL http://www.sciencedirect.com/science/article/pii/S004484860200368X.

Cromey, C.J., Nickell, T.D., Treasurer, J., Black, K.D., Inall, M., 2009. Modelling the impact of cod (*Gadus morhua* L.) farming in the marine environment – codmod. Aquaculture 289 (1–2), 42–53, URL http://www.sciencedirect.com/science/article/pii/S004484860800999X.

Dempster, T., Uglem, I., Sanchez-Jerez, P., Fernandez-Jover, D., Bayle-Sempere, J., Nilsen, R., Bjørn, P., et al., 2009. Coastal salmon farms attract large and persistent aggregations of wild fish: an ecosystem effect. Mar. Ecol. Prog. Ser. 385 (1), 14.

Einen, O., Mørkøre, T., Rørå, A.M.B., Thomassen, M.S., 1999. Feed ration prior to slaughter – a potential tool for managing product quality of Atlantic salmon (*Salmo salar*). Aquaculture 178 (1–2), 149–169, URL http://www.sciencedirect.com/science/article/pii/S004484869900126X.

FAO, 2015. Available from: http://www.fao.org/fishery/statistics/global-aquaculture-production/en. URL http://www.fao.org/figis/servlet/SQServlet?file=/work/FIGIS/prod/webapps/figis/temp/hqp_241118031620595200.xml&outtype=html.

Fenderson, O., Everhart, W., Muth, K., 1968. Comparative agonistic and feeding behavior of hatchery-reared and wild salmon in aquaria. J. Fish. Board Can. 25 (1), 1–14.

Fernandez-Jover, D., Jimenez, J.A.L., Sanchez-Jerez, P., Bayle-Sempere, J., Casalduero, F.G., Lopez, F.J.M., Dempster, T., 2007. Changes in body condition and fatty acid composition of wild Mediterranean horse mackerel (*Trachurus mediterraneus*, steindachner, 1868) associated to sea cage fish farms. Mar. Environ. Res. 63 (1), 1–18.

Findlay, R.H., Watling, L., 1994. Toward a process level model to predict the effects of salmon net-pen aquaculture on the benthos. In: Hargrave, B.T. (Ed.), Modelling Benthic Impacts of Organic Enrichment from Marine Aquaculture. Can. Tech. Rep. Fish. Aquat. Sci., 1949: xi + 125 p.

Forbes, C., Evans, M., Hastings, N., Peacock, B., 2011. Statistical Distributions. John Wiley & Sons.

Føre, M., Dempster, T., Alfredsen, J.A., Johansen, V., Johansson, D., 2009. Modelling of Atlantic salmon (*Salmo salar* L.) behaviour in sea-cages: a lagrangian approach. Aquaculture 288 (3–4), 196–204, URL http://www.sciencedirect.com/science/article/pii/S0044848608008533.

Gillibrand, P., Turrell, W., 1997. Simulating the dispersion and settling of particulate material and associated substances from salmon farms. Tech. rep., Marine Laboratory, Aberdeen, Report No. 3/97, Victoria Road, Aberdeen AB11 9DB, UK.

Gjøsæter, J., Otterå, H., Slinde, E., Nedreaas, K., Ervik, A., 2008. Effekter av spillfôr på marine organismer. Kyst og Havbruk, 52–55 (in Norwegian).

Jobling, M., 1985. Physiological and social constraints on growth of fish with special reference to Arctic charr, *Salvelinus alpinus* L. Aquaculture 44 (2), 83–90, URL http://www.sciencedirect.com/science/article/pii/0044848685900110.

Johansen, S., Jobling, M., 1998. The influence of feeding regime on growth and slaughter traits of cage-reared Atlantic salmon. Aquacult. Int. 6 (1), 1–17.

Juell, J.-E., 1995. The behaviour of Atlantic salmon in relation to efficient cage-rearing. Rev. Fish Biol. Fish. 5, 320–335, http://dx.doi.org/10.1007/BF00043005.

López-Olmeda, J., Noble, C., Sánchez-Vázquez, F., 2012. Does feeding time affect fish welfare? Fish Physiol. Biochem. 38 (1), 143–152, http://dx.doi.org/10.1007/s10695-011-9523-y.

MATLAB, 2014. version 8.4.0.150421 (R2014b). The MathWorks Inc., Natick, Massachusetts.

McDonald, J.H., 2009. Handbook of Biological Statistics, vol. 2. Sparky House Publishing, Baltimore, MD.

McDonald, J.H., 2014. Handbook of Biological Statistics. Sparky House Publishing, Baltimore, MD, URL http://www.biostathandbook.com/kruskalwallis.html.

Noble, C., Kadri, S., Mitchell, D.F., Huntingford, F.A., 2007. Influence of feeding regime on intraspecific competition, fin damage and growth in 1+ Atlantic salmon parr (*Salmo salar* L.) held in freshwater production cages. Aquacult. Res. 38 (11), 1137–1143, http://dx.doi.org/10.1111/j.1365-2109.2007.01777.x.

Noble, C., Kadri, S., Mitchell, D.F., Huntingford, F.A., 2008. Growth, production and fin damage in cage-held 0+ Atlantic salmon pre-smolts (*Salmo salar* L.) fed either (a) on-demand, or (b) to a fixed satiation–restriction regime: data from a commercial farm. Aquaculture 275 (1), 163–168, URL http://www.sciencedirect.com/science/article/pii/S0044848608000069.

Noble, C., Mizusawa, K., Suzuki, K., Tabata, M., 2007. The effect of differing self-feeding regimes on the growth, behaviour and fin damage of rainbow trout held in groups. Aquaculture 264 (1–4), 214–222, URL http://www.sciencedirect.com/science/article/pii/S0044848606009276.

Norwegian Directorate of Fisheries, 2013. Lønnsomhetsundersøkelse for matfiskproduksjon, URL http://www.fiskeridir.no/statistikk/akvakultur/loennsomhet/matfiskproduksjon-laks-og-regnbueoerret.

Oehme, M., Aas, T.S., Sørensen, M., Lygren, I., Åsgård, T., 2012. Feed pellet distribution in a sea cage using pneumatic feeding system with rotor spreader. Aquacult. Eng. 51, 44–52, URL http://www.sciencedirect.com/science/article/pii/S0144860912000568.

Oppedal, F., Dempster, T., Stien, L.H., 2011. Environmental drivers of Atlantic salmon behaviour in sea-cages: a review. Aquaculture 311 (1–4), 1–18, URL http://www.sciencedirect.com/science/article/pii/S0044848610007933.

Osborne, J., 2002. Notes on the use of data transformations. Pract. Assess. Res. Eval. 8 (6).

Pond, S., Pickard, G.L., 1983. Introductory Dynamical Oceanography, 2nd ed. Butterworth-Heinemann, Oxford, ISBN 0-7506-2496-5.

Rasmussen, R.S., Larsen, F.H., Jensen, S., 2007. Fin condition and growth among rainbow trout reared at different sizes, densities and feeding frequencies in high-temperature re-circulated water. Aquacult. Int. 15, 97–107, http://dx.doi.org/10.1007/s10499-006-9070-1.

Ruzzante, D.E., 1994. Domestication effects on aggressive and schooling behavior in fish. Aquaculture 120, 1–24, URL http://www.sciencedirect.com/science/article/pii/0044848694902178.

Ryer, C.H., Olla, B.L., 1996. Growth depensation and aggression in laboratory reared coho salmon: the effect of food distribution and ration size. J. Fish Biol. 48 (4), 686–694, http://dx.doi.org/10.1111/j.1095-8649.1996.tb01464.x.

Skøien, K.R., Alver, M.O., Alfredsen, J.A., 2014. A computer vision approach for detection and quantification of feed particles in marine fish farms. In: IEEE International Conference on Image Processing (ICIP), October 2014, pp. 1648–1652.

Skøien, K.R., Alver, M.O., Alfredsen, J.A., 2015. Modelling spatial surface pellet distribution from rotary pneumatic feed spreaders. In: Proceedings of the 23rd Mediterranean Conference on Control and Automation.

Skøien, K.R., Alver, M.O., Lundregan, S., Frank, K., Alfredsen, J.A., 2016. Effects of wind on surface feed distribution in sea cage aquaculture: a simulation study. In: European Control Conference ECC16.

Skretting, 2012. Fôr. Tech. rep., Skretting (in Norwegian).

Sørensen, M., 2012. A review of the effects of ingredient composition and processing conditions on the physical qualities of extruded high-energy fish feed as measured by prevailing methods. Aquacult. Nutr. 18 (3), 233–248, http://dx.doi.org/10.1111/j.1365-2095.2011.00924.x.

SPSS, 2015. IBM SPSS Statistics for Mac, Version 23.0. Released 2015. IBM Corp., Armonk, NY.

Sutherland, T., Amos, C., Ridley, C., Droppo, I., Petersen, S., 2006. The settling behaviour and benthic transport of fish feed pellets under steady flows. Estuaries Coasts 29 (5), 810–819, URL http://eprints.soton.ac.uk/44121/.

Symons, P.E.K., 1971. Behavioural adjustment of population density to available food by juvenile Atlantic salmon. J. Anim. Ecol. 40 (3), 569–587, URL http://www.jstor.org/stable/3438.

Talbot, C., 1993. Some biological and physical constraints to the design of feeding regimes for salmonids in intensive cultivation. In: Reinertsen, H., Dahle, A.A., Jùrgensen, L., Tvinnereim, K. (Eds.), Fish Farming Technology. Balkema, Rotterdam, pp. 19–26.

Talbot, C., Corneillie, S., Korsøen, Ø., 1999. Pattern of feed intake in four species of fish under commercial farming conditions: implications for feeding management. Aquacult. Res. 30 (7), 509–518, http://dx.doi.org/10.1046/j.1365-2109.1999.00369.x.

Ytrestøyl, T., Aas, T., Berge, G., Hatlen, B., Sørensen, M., Ruyter, B., Thomassen, M., Hognes, E., Ziegler, F., Sund, V., et al., 2011. Resource utilisation and eco-efficiency of Norwegian salmon farming in 2010. Nofima Rep. 53 (2011), 65.